

Pressure-temperature-time path discontinuity in the Main Central thrust zone, central Nepal

Matthew J. Kohn*

Department of Geological Sciences, University of South Carolina, Columbia, South Carolina 29208, USA

Elizabeth J. Catlos

Department of Earth and Space Sciences, University of California, Los Angeles, California 90095, USA

Frederick J. Ryerson

Institute for Geophysics and Planetary Physics, Lawrence Livermore National Laboratory, Livermore, California 94550, USA

T. Mark Harrison

Department of Earth and Space Sciences, University of California, Los Angeles, California 90095, USA

ABSTRACT

Metapelites collected in central Nepal reveal a discontinuity in metamorphic pressure-temperature-time (P - T - t) paths near the base of the Main Central thrust zone, despite an absence of obvious structural breaks. Garnets in the structurally lowest rocks grew with increasing T and P (loading), whereas garnets 1–3 km upsection grew with increasing T , but decreasing P (exhumation). Monazite grains in structurally lower rocks yield ion-microprobe Th-Pb ages of 8–9 Ma. Structurally higher monazite grains range from 10 to 22 Ma. The P - T - t paths confirm previous interpretations that footwall metamorphism in part resulted from thrust reactivation ca. 8 Ma, but also reflect thermal relaxation following older (20 Ma or older) thrust movement. The Main Central thrust zone formed during pulses of movement that resulted in progressive transfer of material from the lower to upper plate.

Keywords: Himalaya, P - T - t paths, geothermometry, geobarometry, geochronology.

INTRODUCTION

The Main Central thrust is the single largest structure within the Indian plate that has accommodated Indian-Asian convergence: it extends ~2500 km along strike and has been the site of at least 140 and perhaps >600 km of displacement (Schelling and Arita, 1991; Srivastava and Mitra, 1994). One critical feature of the structure is its inverted metamorphic field gradient; rocks that were once >650 °C now overlie rocks that never reached such high temperatures. The pressure-temperature-time (P - T - t) evolution of these rocks is thought to be diagnostic of the overall thermal and mechanical behavior of the orogen (England and Thompson, 1984; Ruppel and Hodges, 1994; Harrison et al., 1998; Huerta et al., 1999), but little headway has been made in determining such paths in Nepal, despite numerous thermobarometric studies (see summaries of Guillot, 1999; Macfarlane, 1999). Herein we describe P - T - t paths from rocks collected from within the Main Central thrust shear zone. These paths discriminate among models for the origin of the inverted metamorphism, but also reveal an unexpected discontinuity. The new data alter our understanding of thrust movement in central Nepal and imply kinematic behavior that can be tested in the Himalaya and elsewhere.

BACKGROUND AND SAMPLES

The Main Central thrust is defined (Heim and Gansser, 1939) by the occurrence of high- T , upper amphibolite facies gneisses (Greater Himalayan Sequence) above lower T , greenschist and amphibolite facies rocks (Lesser Himalayan Sequence). The thrust is a thick ductile shear zone, with a continuous decrease in metamorphic grade and temperature downward (e.g., Arita, 1983; Pêcher, 1989). Models proposed for the apparent grade and temperature inversions in central Nepal include (1) premetamorphic to synmetamorphic thrusting (\pm shear heating), followed by thermal relaxation (Le Fort, 1975; Hubbard, 1989; Molnar and England, 1990; Macfarlane, 1995); (2) postmetamorphic thrusting along discrete shear zones (Inger and Harris, 1992; Hubbard, 1996); and (3) continuous synmetamorphic to postmetamorphic shear (e.g., Harrison et al., 1998; Huerta et al., 1998). In general, model 1 implies a clockwise P - T path (including heating with exhumation), model 2 implies prethrusting metamorphic ages and metamorphic repetition, and model 3 implies premetamorphic to synmetamorphic ages and a hairpin P - T path (heating only occurs with loading).

To test these different models, samples were collected in an ~25 km transect along the Darondi River drainage in central Nepal (Fig. 1), representing a structural thickness of ~10

km (Colchen et al., 1986). The contact between the Greater and Lesser Himalayan Sequences is exposed ~2 km south of the northern end of the transect (~1 km structural distance). On the basis of strong top-to-the-south shear senses, we consider all rocks between the Greater Himalayan Sequence and the garnet isograd as part of the Main Central thrust zone. We found no field evidence for any specific structural discontinuities within this zone. Except for differences ascribable to variable protolith composition and competence, all textures and mineral assemblages grade continuously across the transect.

TEXTURES, GARNET ZONING, AND MONAZITE AGES

Samples were investigated for mineral assemblages, textures, compositions, ages, and P - T paths¹. In nearly all samples, a single strong foliation due to isoclinal folding is present. Some lower Lesser Himalayan garnets (e.g., DH-75 and DH-28) have spiral inclusion trails in their cores and overprint the main fabric at their rims, indicating syndeformational to postdeformational garnet growth at that lev-

¹GSA Data Repository item 2001063, Mineral assemblages, textures, compositions, ages, and P - T paths, is available on request from Documents Secretary, GSA, P.O. Box 9140, Boulder, CO 80301-9140, editing @geosociety.org, or at www.geosociety.org/pubs/ft2001.htm.

*E-mail: mjk@geol.sc.edu.

Figure 1. Map showing geology, sample locations (DH-prefix omitted for clarity), and metamorphic isograds along Darondi River valley. Geology of outlying areas is not shown. Contact between upper and lower parts of Lesser Himalayan Sequence separates lithologically dissimilar schists. Strike and dip symbols are representative of foliation orientations for upper and lower sections; middle section is nearly flat structurally. Location of Main Central thrust (MCT) fault is based on lithologic contrasts (Colchen et al., 1986). We define Main Central thrust zone to include all rocks between garnet isograd (DH-16) and end of traverse (DH-63). Mineral isograds are based on thin-section observations. Upper left inset shows cross section along transect. Lower right inset shows outline of Nepal, with approximate locations of Main Central thrust and Darondi River; K is Kathmandu.

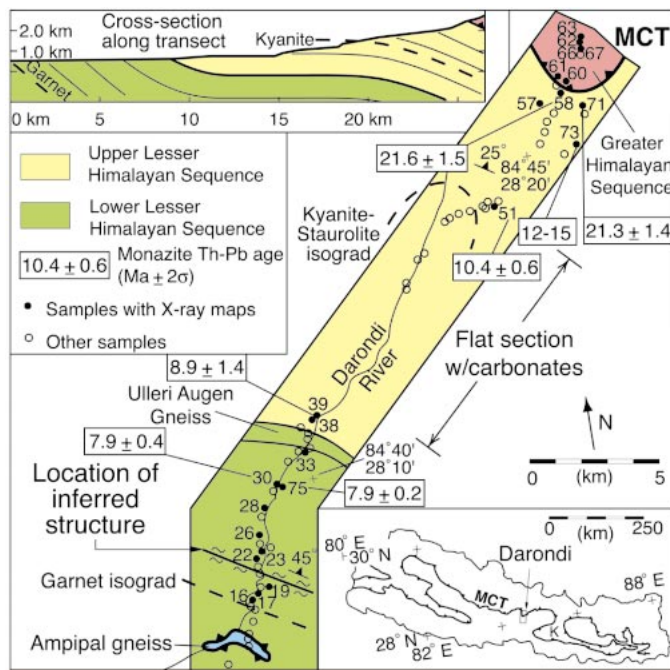


Figure 2. X-ray element maps of Darondi section garnets. Scale bars represent 500 μm . Numbers refer to mole fractions $X_{\text{grossular}}$ and $X_{\text{anorthite}}$ (in garnet [Grt] and plagioclase [Pl] in Ca maps, upper row) and $X_{\text{spessartine}}$ (in garnet in Mn maps, lower row). Generally, lowest Mn values correspond to lowest Fe/(Fe + Mg) and come from highest temperature (T) parts of garnet preserved. Lesser Himalayan Sequence garnets show broad decreases in Mn and Fe/(Fe + Mg) outward from cores, as expected for growth zonation with increasing T (Spear et al., 1990). Samples from uppermost Lesser Himalayan Sequence preserve growth zoning, but also show sharp increase in Mn and Fe/(Fe + Mg) at rim (e.g., DH-58), indicating some garnet resorption and back diffusion of Mn after maximum T was achieved. In Greater Himalayan Sequence, unzoned garnet cores and general rimward increase in Mn and Fe and decrease in Mg indicate high- T diffusional homogenization coupled with significant retrograde reaction and diffusion during cooling. For most samples, minimum Mn and Fe/(Fe + Mg) compositions are appropriate for estimating peak pressure-temperature (P - T) conditions. By collecting X-ray maps prior to fully quantitative microprobe analysis, analytical spots are known to represent lowest Mn and Fe/(Fe + Mg) values and hence permit best estimate of peak P - T conditions for each sample. Distances below X-ray maps show structural location above (positive) or below (negative) contact between Greater Himalayan Sequence and Lesser Himalayan Sequence.

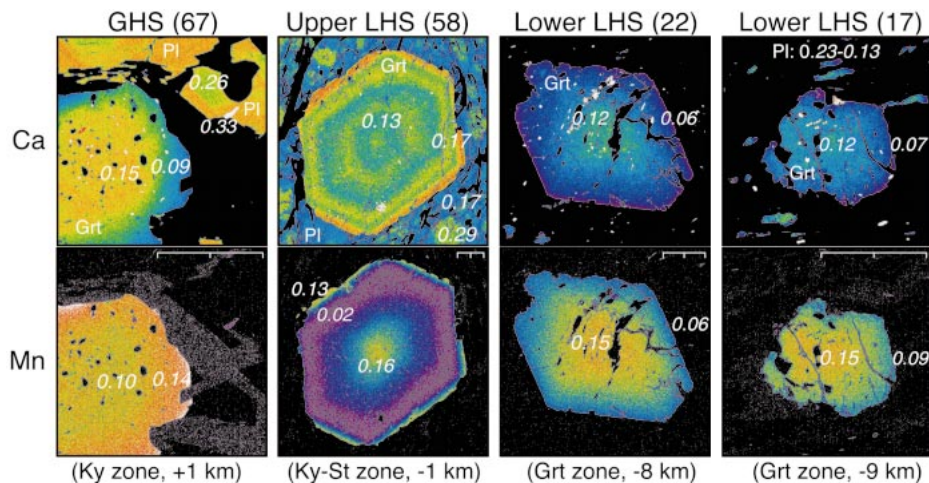


Figure 2. X-ray element maps of Darondi section garnets. Scale bars represent 500 μm . Numbers refer to mole fractions $X_{\text{grossular}}$ and $X_{\text{anorthite}}$ (in garnet [Grt] and plagioclase [Pl] in Ca maps, upper row) and $X_{\text{spessartine}}$ (in garnet in Mn maps, lower row). Generally, lowest Mn values correspond to lowest Fe/(Fe + Mg) and come from highest temperature (T) parts of garnet preserved. Lesser Himalayan Sequence garnets show broad decreases in Mn and Fe/(Fe + Mg) outward from cores, as expected for growth zonation with increasing T (Spear et al., 1990). Samples from uppermost Lesser Himalayan Sequence preserve growth zoning, but also show sharp increase in Mn and Fe/(Fe + Mg) at rim (e.g., DH-58), indicating some garnet resorption and back diffusion of Mn after maximum T was achieved. In Greater Himalayan Sequence, unzoned garnet cores and general rimward increase in Mn and Fe and decrease in Mg indicate high- T diffusional homogenization coupled with significant retrograde reaction and diffusion during cooling. For most samples, minimum Mn and Fe/(Fe + Mg) compositions are appropriate for estimating peak pressure-temperature (P - T) conditions. By collecting X-ray maps prior to fully quantitative microprobe analysis, analytical spots are known to represent lowest Mn and Fe/(Fe + Mg) values and hence permit best estimate of peak P - T conditions for each sample. Distances below X-ray maps show structural location above (positive) or below (negative) contact between Greater Himalayan Sequence and Lesser Himalayan Sequence.

el. However, in most samples garnets crosscut the main foliation, yet also have weak pressure shadows, or have the foliation gently warped around them, indicating both predeformational and postdeformational growth.

X-ray compositional maps of Ca, Fe, Mn, and Mg in garnet were collected from six Greater Himalayan Sequence rock samples and 17 Lesser Himalayan Sequence rock samples. Mn-Fe-Mg zoning trends are consistent with prograde growth in structurally low garnets and with increasing T and retrograde metamorphic reactions at higher levels (Fig. 2). The shift from preservation to eradication of growth zoning (Fig. 2) is an excellent petrologic marker of the Lesser and Greater Himalayan sequence contact. Ca distributions show smooth decreases toward garnet rims in the lower Lesser Himalaya, but patchy or oscillatory zoning in samples in the upper Lesser Himalaya. Most rocks from the lower Lesser Himalaya probably went through a simple reaction and P - T history, and their P - T paths are readily decipherable. However, other samples record either a more complicated reaction and/or P - T history (upper Lesser Himalaya) or diffusional loss of original zonation (Greater Himalaya). Similar zoning patterns across the Main Central thrust north of Kathmandu were described by Fraser et al. (2000).

Th-Pb ages for six Lesser Himalayan Sequence samples were determined in situ from monazite inclusions in garnet and from matrix grains by using a CAMECA IMS 1270 ion microprobe (see Harrison et al., 1995). Monazite inclusion ages are ca. 12–22 Ma at ~ 1 km below the Greater Himalayan Sequence, ca. 9–10 Ma in two other upper Lesser Himalayan samples, and ca. 8 Ma in two lower Lesser Himalayan samples ~ 1 km below the contact between the upper and lower Lesser Himalayan Sequence (Fig. 1). Matrix monazites are ~ 1 m.y. younger than inclusions in garnet, consistent with Pb loss or subsequent growth of matrix grains after inclusions were shielded from Pb loss. Diffusion rates for Pb in monazite (Smith and Giletti, 1997) suggest that on time scales ≤ 10 m.y., and at $T \leq 550$ $^{\circ}\text{C}$, little diffusional reequilibration should occur in 20–50- μm -diameter monazite grains. However, metamorphic monazite occurs in garnet-zone rocks and so can grow at temperatures as low as ~ 500 $^{\circ}\text{C}$. Our age data are consistent with initial metamorphism of the Lesser Himalayan Sequence at or before 20 Ma and continued metamorphic overprinting or reequilibration to ca. 8 Ma.

THERMOBAROMETRY AND P - T PATHS

Thermobarometry indicates a systematic increase in peak P - T conditions from ~ 525 $^{\circ}\text{C}$ and ~ 5 –6 kbar at the base of the transect, to

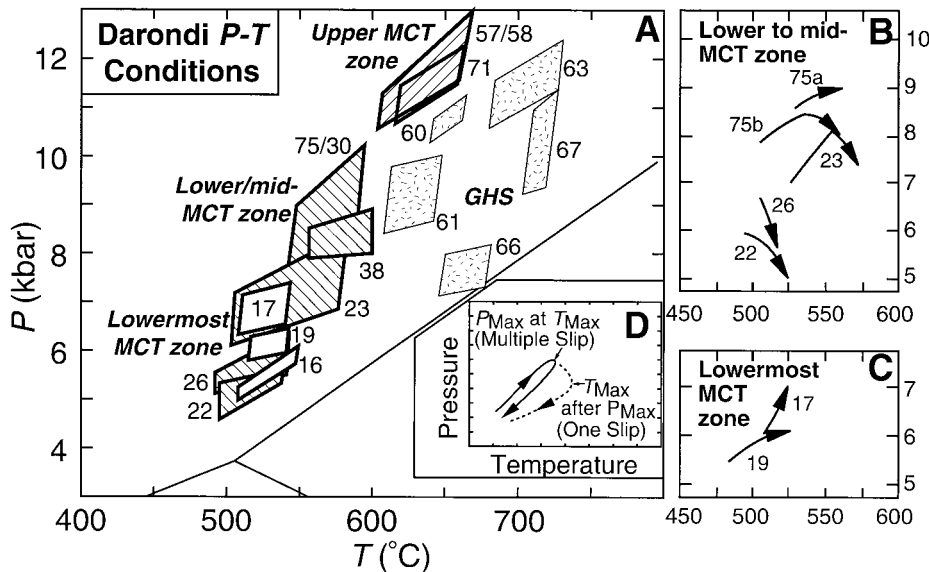


Figure 3. Pressure vs. temperature (P , T) plots for rocks collected along Darondi River traverse. **A:** Within Main Central thrust (MCT) zone, P - T conditions increase toward Greater Himalayan Sequence. Thermobarometers are from Ferry and Spear (1978), Berman (1990), Graham and Powell (1984, DH-38 only), Kohn and Spear (1990, DH-38 only), and Hoisch (1990), and are internally consistent; different recent calibrations change estimated P and T by $\sim \pm 25^\circ\text{C}$ and $\sim \pm 0.5$ – 1 kbar, but do not alter overall trends. **B:** Structurally higher rocks show P - T paths that decrease in P with increasing T . **C:** Structurally lowest rocks show paths that increase in both P and T . P - T paths were based on approach of Spear and Selverstone (1983) and Spear (1993). See footnote 1 for data and details. **D:** P - T path predictions of Lesser Himalayan Sequence samples if one-slip event occurs along single Main Central thrust fault (dashed line) or if multiple-slip events occur within ~ 10 -km-thick shear zone (solid line; Harrison et al., 1998). In latter, Lesser Himalayan Sequence rocks are first buried as slip occurs above them, then transferred to upper plate (still at depth), and finally exhumed and cooled as zone of slip progressively moves to lower structural level.

$\sim 625^\circ\text{C}$ and ~ 11 – 12 kbar near the contact with the Greater Himalaya, ~ 8 km structurally upward (Fig. 3). These results are the first clear documentation that P increases upsection within the Lesser Himalayan Sequence, which contrasts markedly with several previous studies that inferred the opposite trend (e.g., Hubbard, 1989; Macfarlane, 1995; Vannay and Hodges, 1996). The apparent baric gradient excludes any possibility of an intact crustal cross section and implies some component of postmetamorphic shearing. The continuity of P - T conditions along the traverse implies distributed shear rather than major discrete shear surfaces. Greater Himalayan rocks yield more scattered P and T values of 625 – 725°C and 7 – 11 kbar. Evaluation of retrograde reactions and diffusional homogenization of Greater Himalayan garnets indicates that P - T estimates are minima. Compositional homogenization of Greater Himalayan garnets supports either a higher T or longer time at elevated T compared to the Lesser Himalayan rocks.

P - T paths were determined only with lower Lesser Himalayan Sequence rocks because their garnet and plagioclase grains show regular and easily interpretable prograde zonation. Other garnets from the transect either were compositionally homogenized after growth, or grew in an inappropriate mineral assemblage (i.e., lacking plagioclase). All gar-

nets used for P - T path calculations grew in an assemblage containing biotite and chlorite as Fe-Mg minerals. At the base of the transect, DH-17 and DH-19 garnets grew during an increase in both P and T ; however, samples DH-22, DH-23, DH-26, and DH-75 (structurally 1–3 km higher) record little change in P or a decrease in P toward peak T .

INTERPRETATIONS

Main Central thrust movement has been complex, with movement ca. 20–25 Ma (Hodges et al., 1996; Coleman, 1998) and ca. 6–8 Ma (Harrison et al., 1997). Two episodes of movement are consistent with monazite ages of ca. 21 Ma in the structurally highest samples and ca. 8 Ma in lower rocks. One explanation for the metamorphic and age distributions involves progressive underplating of material to the hanging wall during the later phase of thrust movement with thermal and mechanical activation of progressively lower rocks in the sequence (Harrison et al., 1998). The Main Central thrust zone then encompasses all the highly deformed rocks between at least the garnet isograd and the top of the transect in the Greater Himalaya. The predicted P - T path shows a “hairpin”: an increase in both P and T during loading, followed by a decrease in both P and T during exhumation (Fig. 3D; Harrison et al., 1998). Garnet gen-

erally only grows during heating in the observed assemblages (Spear et al., 1990), thereby recording only the loading part of a hairpin path. This model explains the structurally lowest P - T paths that show only heating with loading, and implies significant shearing as much as 8 km below the Greater and Lesser Himalayan sequence contact.

In contrast to the lowest rocks, P - T - t paths of the structurally higher rocks show exhumation during heating. This result is surprising because (1) it is difficult to explain how such different paths can occur within 1 km of each other without an obvious structural break and (2) it suggests either a different history of thrusting for the higher rocks or an unusual thermal structure. Our preferred interpretation is that the paths determined from the higher rocks are the response to loading from early Miocene movement on the Main Central thrust (Harrison et al., 1998). After the early Miocene thickening and perturbation of isotherms, slowing of movement along the fault zone or quiescence until 8 Ma allowed isotherms to relax and the rocks to continue heating conductively. Postthrusting erosion or extension along the higher level South Tibetan detachment system caused pressure to decrease. This interpretation is supported by ca. 21–22 Ma monazite ages from the uppermost Lesser Himalayan rocks, and by textural overprinting of the main fabric by some Lesser Himalayan garnet rims. Heating continued until ca. 6–8 Ma and renewal of rapid movement along the Main Central thrust, so that relatively young monazites in samples DH-30 and DH-75 grew toward the end of quiescence. Structurally higher samples, heated by prior tectonism, had already cooled by the time lower samples reached peak conditions (e.g., DH-71 vs. DH-75, and DH-75 vs. DH-19). Cooling prevented continued reaction and re-equilibration of P - T - t conditions in higher level rocks as the locus of displacement moved progressively down section. This interpretation also implies a significant, yet texturally and structurally cryptic break between DH-19 and DH-22, coinciding with the discontinuity in metamorphic P - T paths.

Alternatively, the exhumation paths may somehow directly reflect 6–8 Ma thrust movement and loading of DH-19 and DH-17, which would require local hanging-wall heating during thrusting and exhumation. High radiogenic heat coupled with continuous accretion and erosion over many tens of million years might result in an inverted thermal gradient (Huerta et al., 1998), and be preserved as an inverted metamorphic gradient. However, this model implies exposure of crustal depths, which are not observed, fails to explain the synchronicity of leucogranite intrusions along the thrust, and requires continuous movement (see Harrison

et al., 1998). Shearing also provides heat (England et al., 1992), but the differential stress required to produce the observed gradient (≥ 1 kbar) far exceeds likely rock strengths for the observed conditions (Engelder, 1993; Kong et al., 1997). Thus, whereas local hanging-wall heating is theoretically possible, we do not believe it is justifiable for the Main Central thrust.

Models for movement along the Main Central thrust that invoke only premetamorphic or synmetamorphic thrusting (model 1) fail to account for the co-occurrence of *P-T* paths in structurally higher rocks that show heating with exhumation and *P-T* paths in structurally low rocks that show heating with loading, or for higher *P* values at higher structural levels. Models that invoke only postmetamorphic thrusting (model 2) do not explain contrasting *P-T* paths and cannot account for metamorphic monazite ages that are either coeval with or postdate movement on the Main Central thrust or the continuous changes in metamorphic grade and *P-T* conditions along the transect. Furthermore, none of these models explains the diachroneity of metamorphism in the upper versus lower parts of the Main Central thrust zone. Instead, continuous synmetamorphic to postmetamorphic shear (model 3) and juxtaposition of at least two distinct metamorphic packages explain better the petrologic and geochronologic data. Testing the validity and generality of our results is best accomplished by combining *P-T* path and *T-t* studies, in which compositional zoning and metamorphic reactions that are well located in *P-T* space are precisely linked to time.

ACKNOWLEDGMENTS

Funded by University of South Carolina, a grant from the Department of Energy's Office of Basic Energy Sciences at Lawrence Livermore National Laboratory under the auspices of contract W-7405-Eng-48, Institute for Geophysics and Planetary Physics, Livermore, and National Science Foundation grants EAR-0073803 (to Kohn) and EAR-9614869 (to Harrison). Reviews by J. Goodge and R. Jamieson improved the manuscript. Field assistance from B.N. Upreti and A. Yin is appreciated.

REFERENCES CITED

Arita, K., 1983, Origin of the inverted metamorphism of the Lower Himalayas, central Nepal: *Tectonophysics*, v. 95, p. 43–60.
 Berman, R.G., 1990, Mixing properties of Ca-Mg-Fe-Mn garnets: *American Mineralogist*, v. 75, p. 328–344.
 Colchen, M., Le Fort, P., and Pêcher, A., 1986, Recherches géologiques dans l'Himalaya du Nepal, Annapurna; Manaslu, Ganesh Himal: Centre National de la Recherche Scientifique, Notice de la carte géologique au 1:200 000, p. 137.
 Coleman, M.E., 1998, U-Pb constraints on Oligocene-Miocene deformation and anatexis within the central Himalaya, Marsyandi Valley, Nepal: *American Journal of Science*, v. 298, p. 553–571.
 Engelder, T., 1993, Stress regimes in the lithosphere:

Princeton, New Jersey, Princeton University Press, 457 p.
 England, P.C., and Thompson, A.B., 1984, Pressure-temperature-time paths of regional metamorphism: Part I. Heat transfer during the evolution of regions of thickened continental crust: *Journal of Petrology*, v. 25, p. 894–928.
 England, P., Le Fort, P., Molnar, P., and Pêcher, A., 1992, Heat sources for Tertiary metamorphism and anatexis in the Annapurna-Manaslu region, central Nepal: *Journal of Geophysical Research*, v. 97, p. 2107–2128.
 Ferry, J.M., and Spear, F.S., 1978, Experimental calibration of the partitioning of Fe and Mg between biotite and garnet: *Contributions to Mineralogy and Petrology*, v. 66, p. 113–117.
 Fraser, G., Worley, B., and Sandiford, M., 2000, High-precision geothermobarometry across the High Himalayan metamorphic sequence, Langtang Valley, Nepal: *Journal of Metamorphic Geology*, v. 18, p. 665–681.
 Graham, C.M., and Powell, R., 1984, A garnet-hornblende geothermometer: Calibration, testing, and application to the Pelona Schist, southern California: *Journal of Metamorphic Geology*, v. 2, p. 13–21.
 Guillot, S., 1999, An overview of the metamorphic evolution in central Nepal: *Journal of Asian Earth Sciences*, v. 17, p. 713–725.
 Harrison, T.M., McKeegan, K.D., and Le Fort, P., 1995, Detection of inherited monazite in the Manaslu leucogranite by $^{208}\text{Pb}/^{232}\text{Th}$ ion microprobe dating: Crystallization age and tectonic significance: *Earth and Planetary Science Letters*, v. 133, p. 271–282.
 Harrison, T.M., Ryerson, F.J., Le Fort, P., Yin, A., Lovera, O.M., and Carlos, E.J., 1997, A late Miocene-Pliocene origin for the central Himalayan inverted metamorphism: *Earth and Planetary Science Letters*, v. 146, p. E1–E7.
 Harrison, T.M., Grove, M., Lovera, O.M., and Carlos, E.J., 1998, A model for the origin of Himalayan anatexis and inverted metamorphism: *Journal of Geophysical Research*, v. 103, p. 27 017–27 032.
 Heim, A., and Gansser, A., 1939, Central Himalaya: Geological observations of the Swiss expedition 1936, Volume 73, p. 245.
 Hodges, K.V., Parrish, R.R., and Searle, M.P., 1996, Tectonic evolution of the central Annapurna Range, Nepalese Himalayas: *Tectonics*, v. 15, p. 1264–1291.
 Hoisch, T.D., 1990, Empirical calibration of six geobarometers for the mineral assemblage quartz + muscovite + biotite + plagioclase + garnet: *Contributions to Mineralogy and Petrology*, v. 104, p. 225–234.
 Hubbard, M.S., 1989, Thermobarometric constraints on the thermal history of the Main Central thrust zone and Tibetan slab, eastern Nepal Himalaya: *Journal of Metamorphic Geology*, v. 7, p. 19–30.
 Hubbard, M.S., 1996, Ductile shear as a cause of inverted metamorphism: Example from the Nepal Himalaya: *Journal of Geology*, v. 104, p. 493–499.
 Huerta, A.D., Royden, L.H., and Hodges, K.V., 1998, The thermal structure of collisional orogens as a response to accretion, erosion, and radiogenic heating: *Journal of Geophysical Research*, v. 103, p. 15 287–15 302.
 Huerta, A.D., Royden, L.H., and Hodges, K.V., 1999, The effects of accretion, erosion and radiogenic heat on the metamorphic evolution of collisional orogens: *Journal of Metamorphic Geology*, v. 17, p. 349–366.
 Inger, S., and Harris, N.B.W., 1992, Tectonothermal

evolution of the High Himalayan crystalline Sequence, Langtang Valley, northern Nepal: *Journal of Metamorphic Geology*, v. 10, p. 439–452.
 Kohn, M.J., 1993, Uncertainties in differential thermodynamic (Gibbs method) *P-T* paths: *Contributions to Mineralogy and Petrology*, v. 113, p. 249–261.
 Kohn, M.J., and Spear, F.S., 1990, Two new barometers for garnet amphibolites with applications to southeastern Vermont: *American Mineralogist*, v. 75, p. 89–96.
 Kong, X., Yin, A., and Harrison, T.M., 1997, Evaluating the role of preexisting weaknesses and topographic distributions in the Indo-Asian collision by use of a thin-shell numerical model: *Geology*, v. 25, p. 527–530.
 Le Fort, P., 1975, Himalayas, the collided range: Present knowledge of the continental arc: *American Journal of Science*, v. 275-A, p. 1–44.
 Macfarlane, A.M., 1995, An evaluation of the inverted metamorphic gradient at Langtang National Park, central Nepal Himalaya: *Journal of Metamorphic Geology*, v. 13, p. 595–612.
 Macfarlane, A.M., 1999, The metamorphic history of the crystalline rocks in the high Himalaya, Nepal: Insights from thermobarometric data: *Journal of Asian Earth Sciences*, v. 17, p. 741–753.
 Molnar, P., and England, P.C., 1990, Temperatures, heat flux, and frictional stress near major thrust faults: *Journal of Geophysical Research*, v. 95, p. 4833–4856.
 Pêcher, A., 1989, The metamorphism in the central Himalaya: *Journal of Metamorphic Geology*, v. 7, p. 31–41.
 Ruppel, C., and Hodges, K.V., 1994, Pressure-temperature-time paths from two-dimensional thermal models: Prograde, retrograde, and inverted metamorphism: *Tectonics*, v. 13, p. 17–44.
 Schelling, D., and Arita, K., 1991, Thrust tectonics, crustal shortening and the structure of the far eastern Nepal Himalaya: *Tectonics*, v. 10, p. 851–862.
 Smith, H.A., and Giletti, B.J., 1997, Lead diffusion in monazite: *Geochimica et Cosmochimica Acta*, v. 61, p. 1047–1055.
 Srivastava, P., and Mitra, G., 1994, Thrust geometries and deep structure of the outer and lesser Himalaya, Kumaon and Garwal (India): Implications for evolution of the Himalayan fold-and-thrust belt: *Tectonics*, v. 13, p. 89–109.
 Spear, F.S., 1993, Metamorphic phase equilibria and pressure-temperature-time paths: Washington, D.C., Mineralogical Society of America, 799 p.
 Spear, F.S., and Selverstone, J., 1983, Quantitative *P-T* paths from zoned minerals: Theory and tectonic applications: *Contributions to Mineralogy and Petrology*, v. 83, p. 348–357.
 Spear, F.S., Kohn, M.J., Florence, F., and Menard, T., 1990, A model for garnet and plagioclase growth in pelitic schists: Implications for thermobarometry and *P-T* path determinations: *Journal of Metamorphic Geology*, v. 8, p. 683–696.
 Vannay, J.C., and Hodges, K.V., 1996, Tectonometamorphic evolution of the Himalayan metamorphic core between the Annapurna and Dhaulagiri, central Nepal: *Journal of Metamorphic Geology*, v. 14, p. 635–656.

Manuscript received September 5, 2000

Revised manuscript received March 7, 2001

Manuscript accepted March 19, 2001

Printed in USA